J Mater Sci (2010) 45:3506–3513
DOI 10.1007/s10853-010-4387-6

Modeling and prediction of compressive creep of silane-treated TiO_2/high-density polyethylene

C. X. Dong · S. J. Zhu · M. Mizuno · M. Hashimoto

Received: 4 January 2010 / Accepted: 4 March 2010 / Published online: 19 March 2010

Abstract Silane-treated TiO_2/high-density polyethylene (silane-TiO_2/HDPE) is a potential bone substitute material with good bioactivity and mechanical properties. In this composite, 40 vol.% TiO_2 particles were connected chemically with HDPE (high-density polyethylene) by silane-coupling agent. The intensive silane connection was believed to play very important role in compressive creep behavior of silane-TiO_2/HDPE in our previous study. In order to deeply understand the relationship between the special structure and creep behavior, both a viscoelastic creep model named Burgers, and an empirical model called Findley power law were applied to simulate and predict the creep curves obtained in both air and saline solution. The results showed that Burgers model succeeded in simulating the creep curves but failed in long-term prediction for all dry samples, while Findley power law failed in simulating the creep curves in air but succeeded in saline solution. By analyzing the parameters obtained from Burgers model, it was believed that the structure of intense connection by silane chains resulted in the very big and gradually increased permanent viscous flow of this material with creep time. The big permanent viscous flow brought on the failure in simulating creep curves using Findley power law, and the improved permanent viscous flow during creep conduced to the positive deviation between the prediction and practical creep curve using Burgers model. The effect of saline solution around sample could not only decrease the permanent viscous flow but also stabilize it gradually, which resulted in the success in the prediction and simulation of creep curve in saline solution by the two models.

C. X. Dong · S. J. Zhu (✉)
Department of Intelligent Mechanical Engineering, Fukuoka Institute of Technology, Fukuoka 811-0295, Japan
e-mail: zhu@fit.ac.jp

C. X. Dong
College of Chemistry and Biology, Beihua University, Jilin City 132013, China

M. Mizuno · M. Hashimoto
Japan Fine Ceramics Center, Nagoya 456-8587, Japan

Introduction

With the development of materials science, filling polymer with inorganic particles has been proved to be an effective way in improving the mechanical properties of polymers [1, 2]. In the studies of the polymer composites, filler concentration, dispersion state, and interfacial bonding are considered to be important factors that can significantly influence the properties of bulk materials [3]. Owing to the small size and large interfacial area of nanofillers, low content of the inorganic filler is usually preferred [4]. Meanwhile, in order to improve the dispersion and interfacial bonding, surface modifications of nanofillers with organic chemicals are also widely used [5–8].

In the case of the polymer composites, creep behavior is very important for practical application. However, the complex creep performances of polymer composites can be deeply understood only by combining experimental studies with effective modeling. Modeling and simulation of polymer-based composites have become an essential issue for the development of materials in potential engineering application. Moreover, for some composites potentially used for a long period of service, such as bone substitute biomaterials or engineering composites, the service time is very long, usually longer than the practical experimental time in laboratory. Therefore, prediction based on experimental creep data is also meaningful to get a proper

perspective about the size reliability for long-time loading. Therefore, modeling and prediction are usually carried out in the creep research of polymer composites.

Among the various models, Burgers model and Findley power law are often employed, because the parameters in Burgers model correspond with some physical parameters of materials, which can help us to deeply understand the structural relationship with mechanical properties, and Findley power law is an empirical model, which has been successfully used in many polymer-based composites. For example, Yang et al. [9] simulated the creep curves successfully and predicted the long-term creep behaviors of polyamide 66 composites on the basis of short-time creep data obtained by them. In other studies [10, 11], the creep curves of the polymer composites could also be well modeled by them. However, to our best knowledge, no analytical study has been reported on the reasons for failure, in case one of them fails in simulating or predicting the creep behaviors.

Silane-TiO_2/HDPE is a potential bone substitute biomaterial developed by Hashimoto et al., which has high filler content of 40 vol.% TiO_2 and establishes intense silane connection between TiO_2 and HDPE (1 wt% of silane-coupling agent in modified TiO_2) by forming chemical bonds at both of the ends of the silane chains [12]. As a bone substitute material, it is very important to know its compressive creep behavior during long period of loading. In our previous study, the compressive creep mechanisms and the relationship between intense silane connection and creep behavior were studied and described in detail [13]. The variation of silane chains under loading was inferred to have played a key role in compressive creep behavior. This article presents two macroscopic models, namely, Burgers model and Findley power. The simulation and prediction by these models were carried out to deeply understand the effect of silane connection on the creep behavior of this composite. Furthermore, the reasons for failure in simulating the creep curves using Findley power law and prediction using Burgers model were explored.

Materials and methods

Materials

Silane-treated TiO_2/high-density polyethylene (Silane-TiO_2/HDPE) composite was fabricated in Japan Fine Ceramics Center (Nagoya, Japan). Anatase-type TiO_2 nanopowders were manufactured by Ishihara Sangyo Kaisha (Ltd., Osaka, Japan) with mean particle size of 535 nm. [γ-(methacryloxy)propyl]trimethoxysilane (γ-MPS) was employed (Shin-Etsu Chemical Co. Ltd., Tokyo, Japan). The HDPE (Japan Polyolefins Co. Ltd., Tokyo, Japan) has the number-average molecular weight (Mn) of 1.21×10^4, weight-average molecular weight (Mw) of 7.67×10^4, and z-average molecular weight (Mz) of 47.6×10^4. The ratio of TiO_2 to HDPE is 40 vol.%.

The detailed manufacturing process has been described in literature [12]. First, TiO_2 powders were treated with the silane-coupling agent as follows: 1.1 g of γ-MPS, 1.6 g of ethanol, and 0.2 g of ion-exchanged distilled water were stirred using a magnetic stirrer for 10 min. The solution containing the silane-coupling agent was added to 110 g of TiO_2 powder and mixed in the shaker mixer at 25 °C for 1 h. After mixing, the mixtures were dried and heated at 130 °C for 5 min. Then, the manufacturing of silane-TiO_2/HDPE by kneading and compression molding was carried out as follows: HDPE was dried at 80 °C for 8 h and then kneaded at 210 °C in a batch kneader PBV 0.3 (Irie Shokai, Ltd., Tokyo, Japan). Modified TiO_2 particles with silane-coupling agent were added slowly into the melted HDPE with kneading at 210 °C in air. After adding modified TiO_2, silane-TiO_2/HDPE compound was kneaded at 25 rpm for 30 min. The obtained compounds were molded at 230 °C for 1 h and then hot-pressed in air at a pressure 5 MPa. From the analysis of FTIR, it was believed that the surface of TiO_2 particles was connected with HDPE through formation of Ti–O–Si bonds.

Compressive creep

The specimens of silane-TiO_2/HDPE were cut to cylindrical shape and polished to a diameter of 6 mm and a height of 12 mm. Before creep tests, compressive strength tests were carried out in air and in saline solution at room temperature. The Young's modulus is 2.9 GPa in air and 2.1 GPa in saline solution. Compressive strength is 71 MPa in air and 63 MPa in saline solution. A servo-hydraulic fatigue machine Model EHF-EB5 (Shimadzu Co. Ltd., Japan) was employed. Tests were carried out in air or in saline solution of 0.9% NaCl at 25 °C. The temperature controlling of saline solution was realized by means of pumping and recycling the saline solution of 25 °C into the test trough during the experimental process.

Creep models

Burgers model

Burgers, or four-element, model is widely used to simulate the viscoelasticity of materials. This model includes four essential elements, which can satisfactorily describe the basic variation of bulk material structure. Through the analysis of the modeling parameters, the creep resistance variation arising due to the filling of nanoparticles can be deeply understood.

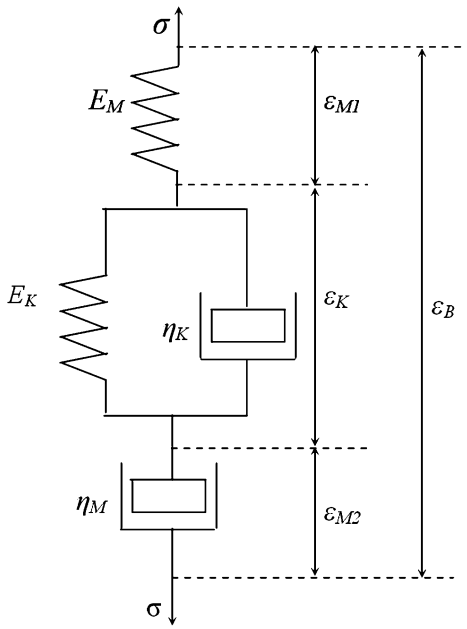

Fig. 1 Schematic illustration of Burgers model

The model includes a Maxwell and a Kelvin unit connected in series, as shown in Fig. 1 [14]. The total creep strain ε_B at time t is the summation of the strains from three elements.

$$\varepsilon_B = \varepsilon_{M1} + \varepsilon_{M2} + \varepsilon_K \quad (1)$$

where the subscripts B, M, and K indicate Burgers model, Maxwell, and Kelvin unit, respectively; ε_{M1}, ε_{M2}, and ε_K represent the strains of the Maxwell spring, Maxwell dashpot, and Kelvin unit, respectively. The creep behavior of Burgers model can be expressed as the following equation:

$$\varepsilon_B = \frac{\sigma_0}{E_M} + \frac{\sigma_0}{E_K}\left(1 - e^{-t/\tau}\right) + \frac{\sigma_0}{\eta_M}t \quad (2)$$

where E_M and η_M are the modulus and viscosity of the Maxwell spring and dashpot, respectively; E_K and η_K are the modulus and viscosity of the Kelvin spring and dashpot, respectively; σ_0 is the initially applied stress; $\tau = \eta_K/E_K$ is the retardation time taken to produce 63.2% or $(1 - e^{-1})$ of the total deformation in the Kelvin unit.

The creep characteristics of Burgers model shown in Eq. 2 can be depicted as follows. The first term is a constant and describes the instantaneous elastic deformation. The second one is delayed elasticity of the Kelvin unit and dominant in the earliest stage of creep. It soon attains a saturation value close to σ_0/E_K; in the third term, the strain then increases nearly linearly after sufficiently long period of loading.

Differentiating Eq. 2 yields the creep rate of Burgers model:

$$\dot{\varepsilon}_B = \frac{\sigma_0}{\eta_M} + \frac{\sigma_0}{\eta_K}e^{-t/\tau} \quad (3)$$

From Eq. 3, it is known that the creep rate decreases with creep time, which means that the Burgers model is not suitable for describing creep behavior with increasing creep rate. The creep rate will reach asymptotically a constant value in the stable creep stage.

Findley power law

Findley power law is an empirical model, which can effectively simulate the creep data of plastics over a wide time scale:

$$\varepsilon_F = \varepsilon_{F0} + \varepsilon_{F1}t^n \quad (4)$$

where the subscript F indicates the parameters associated with the Findley power law, n is a constant independent of stress and generally less than one; ε_{F0} and ε_{F1} are the instantaneous strain and time-dependent coefficient, respectively.

Modeling methods

The creep data were simulated using the Nonlinear Curve Fit function in OriginPro (OriginLab Corporation, USA). During the fitting process, a valid initial value of the parameters should be given. Otherwise, a bad initial value will lead to a non-convergent outcome and make the simulation fail. In this study, the initial values were tried first with the data from literature [9]. Then the obtained valid parameters were used as initial values for other creep curves. After one of the parameters became non-convergent or negative, or the parameter n in Findley power law was greater than 1, the simulation was rejected as invalid. Because all the simulating parameters with Findley power law for almost all the creep curves were invalid except the one tested in saline solution at 45 MPa, another fitting software program 1stopt was employed to testify the obtained values. In 1stopt program, the simulation is performed using Universal Global Optimization (UGO) procedure, in which no initial values of the parameters are needed. The values from Originpro were greatly consistent with those obtained from the program 1stopt.

Results and discussion

Creep rates

Creep rate represents the velocity of creep deformation. The creep rate curves versus creep time under different stress levels are shown in Fig. 2. In air, the start creep rates

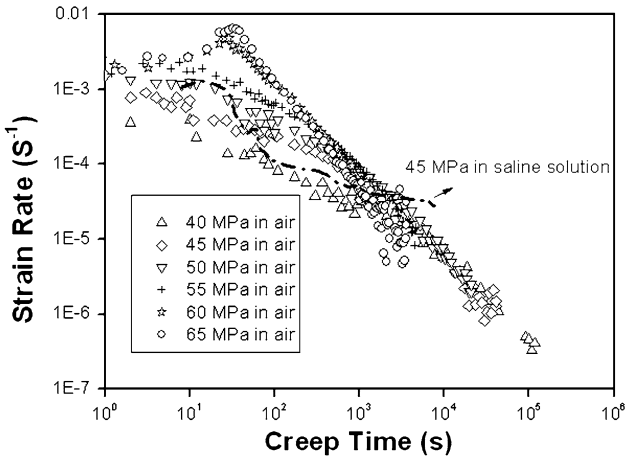

Fig. 2 Creep rate curves versus creep time at different stress levels

at the instant of loading increase with the load stress level up to 50 MPa. Beyond 50 MPa, they remain almost the same. The creep rates under stress lower than 50 MPa all decrease with creep time monotonically, while the creep rates at 60 and 65 MPa increase sharply after about 10 s and soon come down. All the creep curves in air only experienced the first primary stage, and did not attain the steady-state stage. The creep rate at 45 MPa in saline solution is shown by dash line. Clearly, the start creep rate at the beginning of creep is almost the same as that at 45 MPa in air. Then, it remains at this high value for a while, decreases quickly, and remains almost stable after 100 s. It is clear that the creep in saline solution at 45 MPa attained secondary stage.

Based on the creep rate curves, creep mechanisms were proposed and discussed in detail in the previous article of this series [13], in which silane connection has been demonstrated to plays key role. Once stress is loaded, the concentrated compressive stress on the interface between the filler and matrix can destroy the weak mechanical adhesion and be relaxed by stretching the silane chains in the perpendicular direction to the loading axis. Meanwhile, the shear stress on the upper and the bottom layers of the particle surface, which is the consequence of small deformation and reorientation of silane chains, can also stretch other silane chains. The extent of stretching depends on the concentrated stress around the particle. Although under compressive stress the surrounding HDPE has to change in structure to help relieve stress concentrations, compared with silane chains during creep, deformation of HDPE and its effect on creep rate variation are negligible. In saline solution, the actual variation in external shape of specimen should be considered. For polymer composites, when compressed, the central lateral surface will protrude out with the reduction of axial length. With the increase of projection, tensile stress on the lateral surface will come into being and increase gradually. Because of the hydrophilicity of TiO_2 surface, the basis for its bioactivity in biomaterials, once the magnitude of the concentrated stress on sample surface attains a value enough to break the chemical bond of Ti–O–Si, Ti–OH and Si–OH will form subsequently. In air, the forming process is very slow, while in saline solution, the process is accelerated because of the surrounding water. The steric hindrance and repelling force between hydrogen atoms from the introduced –OH in air, and the additional hydrostatic force and steric hindrance from water in saline solution, all can enhance the stress concentrations in return. Because the tensile stress on lateral surface of samples increases gradually with creep process, the effect of saline solution on creep rate should be time dependent. It is very small at creep beginning and becomes gradually remarkable after a period, which is the reason for the almost same creep rate at the creep beginning and comparatively higher creep rate, subsequently.

Creep modeling

For silane-TiO_2/HDPE, the experimental curves of creep strain versus creep time and their corresponding simulated curves from Burgers model (in solid lines) are presented in Fig. 3. The modeling curves fit very well with the corresponding creep curves. Obviously, the load stress has an important effect on the creep behaviors of silane-TiO_2/HDPE. The higher the applied stress the shorter the creep time to rupture, and the severer the dimensional deformation.

In order to manifest the effect of saline solution, the creep curves and corresponding fitting curves in saline solution and in air at 45 MPa are shown in Fig. 4. The fitting curves using Burgers model agree perfectly with the experimental lines. Creep life of silane-TiO_2/HDPE in

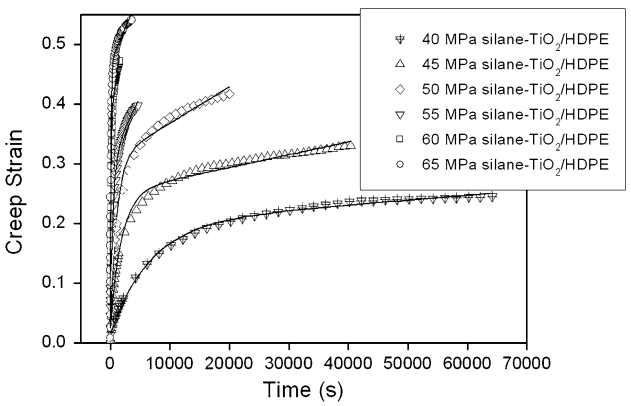

Fig. 3 Modeling results of Burgers model (in *solid lines*) for experimental creep data of silane-TiO_2/HDPE in air under different stress levels

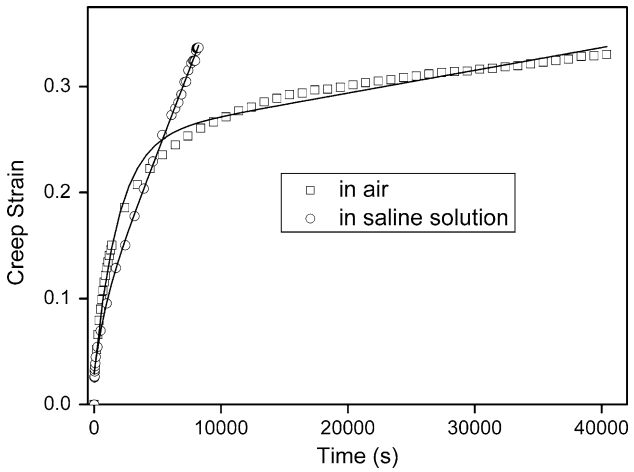

Fig. 4 Modeling results of Burgers model (in *solid lines*) for experimental creep data obtained in saline solution and air at 45 MPa

saline solution is shortened greatly, while the creep strain remains almost the same.

The simulating parameters adopted using Burgers model are shown in Table 1. The variations of E_M and E_K with stress are a little complicated. E_M decreases with an increase in stress from 40 to 55 MPa, while E_K decreases from 40 to 50 MPa. Subsequently, however, they do not show any orderly variation. η_M and η_K decrease quickly with stress enhancement from 40 to 50 MPa, and then the rate of decrease gradually slows down, manifesting that the two viscous flows were all gradually limited after 50 MPa. The retardation time also decreases with load stress, exhibiting that the time needed to reach the total deformation was reduced. In other words, the anti-deformation ability was decreased when applied stress was increased.

From the proposed creep mechanisms, the variations of modeling parameters with stress level can be well understood. In this composite, silane chains were the main amorphous phase. Because of their nonlinear stress–strain response, E_M was decreased when stress level increased in the range of 40–55 MPa. After loading, the destructive extent of silane chains increased with the applied stress enhancement, which resulted in the decrease of stiffness and viscosity of silane chains. The breakage of more silane chains also led to the easier viscous flow between molecular chains of HDPE, and therefore, the shorter time to attain the final deformation. Therefore, E_K, η_K, η_M, and the retardation time τ all decreased with load stress. It should be mentioned that Burgers model does not fit to describe creep with increasing creep rate, and so the modeling parameters after 50 MPa do not follow the trend of decreasing variation.

In saline solution, the instantaneous elastic modulus E_M is almost the same, but the other three parameters are greatly different from the corresponding parameters in air at 45 MPa. E_K and η_K were increased obviously, while η_M and retardation time were greatly decreased. The variations of the parameters in saline solution could be well understood when considering the effect mechanism of saline solution on creep. The very small effect of saline solution at the instant of loading brought on the almost same E_M in saline solution. With a prolonged creep time, saline solution broke more silane chains around crack tips on sample surface compared with dry sample, which slowed down the orientation and stretching movement of silane chains in bulk sample, leading to the reduced elastic deformation and viscous flow within chain segments of HDPE. Therefore, E_K and η_K values in saline solution were increased. The breakage of more silane chains by saline solution on sample surface resulted in the easier permanent viscous flow and the shorter time to attain the final deformation [9]. Therefore, η_M and the retardation time τ in saline solution all decreased compared to the corresponding values in air at 45 MPa.

Findley power law was also used to simulate the creep curves of dry samples, but no valid parameters were obtained. For the creep curve in saline solution at 45 MPa, the three parameters from Findley power law are 0.031, 0.00037, and 0.74 for ε_{F0}, ε_{F1}, and n, respectively. The simulating curve from the three parameters fits very well the creep curve in saline solution (curves are not shown here).

Table 1 Creep parameters of silane-TiO_2/HDPE based on the simulation of Burgers model

Sample and test condition	Stress (MPa)	E_M (MPa)	E_K (MPa)	η_K (GPa s)	η_M (GPa s)	τ (s)
Silane-TiO_2/HDPE in air	40	2315	220	1474	50152	6714
	45	1577	202	376	20942	1858
	50	1318	186	201	8225	1083
	55	993	217	109	2681	505
	60	2426	171	20	895	117
	65	1416	154	18	2762	115
Silane-TiO_2/HDPE in saline solution	45	1481	868	778	1443	896

Prediction of long-term creep

The prediction parameters using Burgers model were determined based on the data of half creep time to rupture for silane-TiO_2/HDPE. The data on later half creep time were obtained from Eq. 2. The experimental data and the predicting lines of dry samples are exhibited in Fig. 5. For the samples tested at 60 and 65 MPa, when creep time was shortened by half, data were not enough to get valid parameters. The solid lines are the simulating and prediction curves. Clearly, the simulating curves fit the creep curves very well at the first half of the creep time, while the predictions show huge positive deviations from the experimental data.

The predictions of creep curve in saline solution at 45 MPa using both Burgers and Findley power law are exhibited in Fig. 6. The predicting parameters were obtained through the same method as the description above. The goodness of predictions by the two models for the later half creep time is exhibited by the coefficient of determination R^2, which is 0.9964 for Burgers model, and 0.9958 for Findley power law (significance level $p < 0.0001$). Obviously, the prediction using Burgers model is very good when compared with the actual creep curve, and Burgers model clearly shows a better prediction than the one using Findley power law.

A question is naturally brought forward: "What determines the validity of the prediction and simulation using Burgers model and Findley power law?" Because the samples tested in saline solution are the same as those in air, it can be concluded that the validity of simulation or prediction relies heavily on the apparent curve profile, which depends on the parameters used in Burgers model. On a comparison of the corresponding parameters, it was found that E_K is the highest and η_M is the lowest for the sample in saline solution at 45 MPa among all the samples. Hence, it is inferred that the second and third terms in Eq. 2 are related.

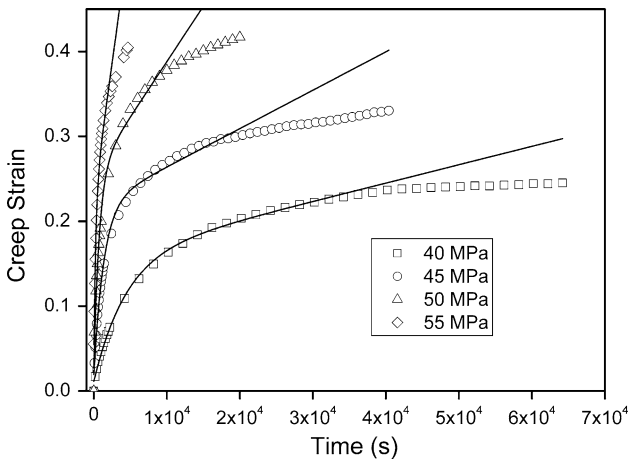

Fig. 5 Prediction using Burgers model at different stresses in air. *Solid lines* are simulating curves based on half of the total creep rupture time, correspondingly

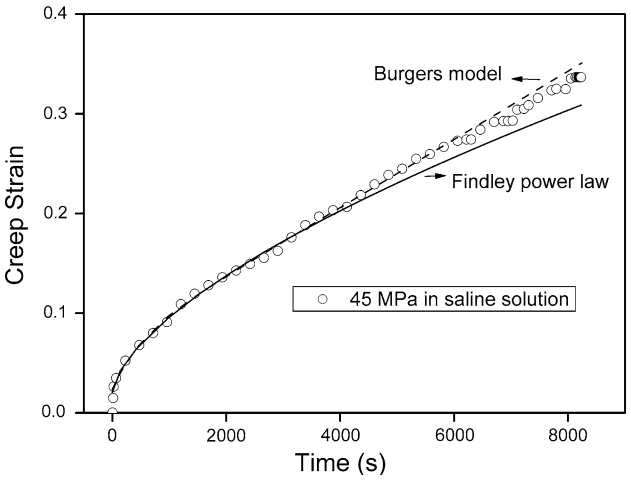

Fig. 6 Prediction using Burgers model and Findley power law for the creep curve obtained in saline solution at 45 MPa. Simulating is based on half of the total creep rupture time

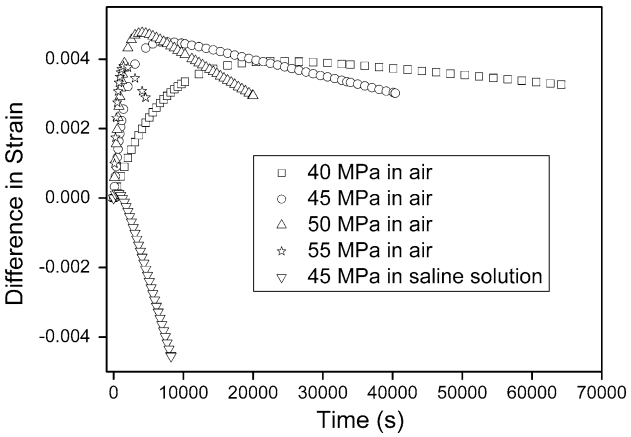

Fig. 7 Strain difference curves between the secondary and tertiary terms in Eq. 2 with creep time

Figure 7 shows the variation curves of the strain difference between the secondary term and the third term in Eq. 2 under the function of creep time. The differences of dry samples are all positive, while most of the differences of sample in saline solution are negative. With creep time prolonged, the differences for all dry samples increase first and then decrease, exhibiting that both E_K and η_M controlled the creep behavior and the creep curves in air do not follow power function. For the curve in saline solution at 45 MPa, the difference increases for very short time and then decreases monotonically, showing that the creep curve in saline solution mainly follows power function. Clearly, whether the strain difference follows power law is determined by the relative magnitude of permanent viscous flow

compared with the corresponding E_K. The permanent viscous flows of dry samples were all very big, while the one in saline solution was obviously small when comparing the corresponding values for E_K. How big the permanent viscous flows of dry samples are can be understood by the comparison with those of other composites. For example, the one of the dry sample at 40 MPa is more than one hundred thousand times higher than those of polyamide 66 nanocomposites (PA) with 1 wt% TiO_2 at the same stress level and room temperature, which is 0.25 GPa s for PA with 21 nm TiO_2 particles and 0.19 GPa s for PA with 300 nm TiO_2 [9]. Therefore, the comparatively big permanent viscous flow is believed to be the main reason for the failure in simulation using Findley power law.

Certainly, the external profiles of creep curves were determined by the inherent structure of this material. That is the intense connection by silane chains between TiO_2 and HDPE. Because the total amounts of silane chains being oriented and stretched in the whole sample due to the gradually protruding deformation of bulk sample under compression, and the stretching extents of the silane chains increased with the prolonged creep time, the permanent viscous flow could also be improved gradually with creep time, which was confirmed by the much smaller $\eta_M s$ obtained with the data of first half creep time compared to the corresponding ones obtained with the total creep data for all the dry samples (data not shown). Because lower constants were used in the prediction for permanent viscous flows in dry samples, the actual enhanced permanent viscous flows during creep resulted in the positive deviations in the predictions of dry samples using Burgers model. In saline solution, because the enhanced breakage of silane connection was accelerated with prolonged creep time, the decreasing effect on the permanent viscous flow was also enhanced with prolonged creep time. When the improvement of permanent viscous flow because of protruding deformation of bulk sample and the decrease of permanent viscous flow because of saline solution attained the equilibrium with prolonged creep time, the permanent viscous flow maintained almost the same state. Therefore, the prediction using Burgers model in saline solution at 45 MPa fits very well with the corresponding practical creep curve.

From the above discussion, it is concluded that the microstructure of composites and the testing condition all play very important role in creep behavior and modeling results. Although the modeling study of compressive creep using Burgers model or Findley power law has not been found for real bone, there are a few articles using other models [15, 16]. Burns et al. [15] studied the compressive creep of intervertebral disks using a three-parameter-solid model, which is composed of a Kelvin unit, a spring connected in series, and a four-parameter-solid model, which consists of two Kelvin-units connected in series. The results exhibited good simulations and predictions. Another study [16] was done based on the Standard Linear Solid, which consists of a spring and a Maxwell unit in parallel with each other. Clearly, there is no comparability between the corresponding parameters obtained from the models used in real bones and the ones from Burgers model used in silane-TiO_2/HDPE. However, the compressive creep curves of bones followed power law [17], which are different from the creep curves of dry silane-TiO_2/HDPE. The difference can also be exhibited by the profiles of creep curves. The bone exhibits classical three-stage creep: a rapid concave-down first stage, a slower but stable second stage, and a fast concave-up third stage [17], whereas the dry silane-TiO_2/HDPE only shows the first stage. From the facts that there is bodily fluid in bone and that the creep of silane-TiO_2/HDPE in saline solution attained the second creep stage, it was inferred that lack of water in dry silane-TiO_2/HDPE could be a possible reason for the above discrepancy of creep behaviors. The inference is consistent with the reports of previous studies proposing that microstructures and compositions of bone can greatly affect the mechanical properties of bone [18, 19].

Conclusions

On the basis of compressive creep data, modeling and prediction of creep behavior of biomaterial silane-TiO_2/HDPE were carried out using both Burgers model and Findley power law. The results showed that Burgers model succeeded in simulating the creeps for the experimental data and failed in the long-term creep prediction for all the dry samples. On the other hand, Findley power law failed in simulating the creep in air but succeeded in saline solution. It was concluded that the structure of intense bonding by silane chains in silane-TiO_2/HDPE played a key role in the creep processes and in the simulations and predictions. The special structure determined the very big and improved permanent viscous flow with prolonged creep time. The big permanent viscous flows brought on the failure in simulation using Findley power law. The improved permanent viscous flows of dry samples with creep time resulted in the higher prediction values obtained while using Burgers model. The existence of saline solution could not only decrease the permanent viscous flow but also make it almost stable during creep time, which induced the success of simulation and prediction by the two models.

References

1. Sheng N, Boyce MC, Parks DM, Rutledge GC, Abes JI, Cohen RE (2004) Polymer 45:487
2. Saeed MB, Zhan M (2007) Int J Adhes Adhes 27:306

3. Fu SY, Feng XQ, Lauke B, Ma YW (2008) Compos B 39:933
4. Yang J-L, Zhang Z, Schlarb AK, Friedrich K (2006) Polymer 47:2791
5. Zhou TH, Ruan WH, Yang JL, Rong MZ, Zhang MQ, Zhang Z (2007) Compos Sci Technol 7:2297
6. Tee DI, Mariatti M, Azizan A, See CH, Chong KF (2007) Compos Sci Technol 67:2584
7. Othman N, Ismail H, Mariatti M (2006) Polym Degrad Stab 91:1761
8. Zhang SM, Liu J, Zhou W, Cheng L, Guo XD (2005) Curr Appl Phys 5:516
9. Yang J-L, Zhang Z, Schlarb AK, Friedrich K (2006) Polymer 47:6745
10. Lietz S, Yang J, Bosch E, Sandler JKW, Zhang Z, Altstädt V (2007) Macromol Mater Eng 292:23
11. Wang ZD, Zha XX (2008) Mater Sci Eng A 486:517
12. Hashimoto M, Takadama H, Mizuno M, Kokubo T (2006) Mater Res Bull 41:515
13. Dong CX, Zhu SJ, Mizuno M, Hashimoto M (2010) J Mater Sci 45:1796. doi:10.1007/s10853-009-4161-9
14. Ward IM (1983) Mechanical properties of solid polymers. Wiley, Chicherster
15. Burns ML, Kaleps I, Kazarian LE (1984) J Biomech 17:113
16. Li SP, Patwardhan AG, Amirouche FML, Havey R, Meade KP (1995) J Biomech 28(7):779
17. Bowman SM, Keaveny TM, Gibson LJ, Hayes WC, McMahon TA (1994) J Biomech 27:301
18. Goldstein SA (1987) J Biomech 20:1055
19. Yerramshetty JS, Akkus O (2008) Bone 42:476